# Development of potential model for radiation damage simulation in α-Fe

Sehyeok Park and Takuji Oda*
*Department of Nuclear Engineering, Seoul National University, 1, Gwanak-ro, Gwanak-gu, Seoul 151-744, Republic of Korea*
**Corresponding author: oda@snu.ac.kr*

## 1. Introduction

Ferritic steels are widely used as components and structural materials in nuclear fission and fusion reactors [1][2]. Therefore, radiation damage processes and effects in ferritic steels has been the subject of extensive studies in decades.

Classical molecular dynamics (CMD) simulations are widely used in this field, because it can treat a large simulation system and long simulation length required to pursue atomic motion during radiation damage processes. In general, the results of CMD simulation are dependent on the potential model used in the simulation. For radiation damage studies, threshold displacement energy (TDE), average number of Frenkel pair (FP) defect and atom displacement cross sections largely depend on the potential model [3].

In radiation damage simulations, it is common practice to join the potential model constructed with equilibrium state properties to the ZBL potential model, which is designed for atomic collision processes, using an arbitrary function. This arbitrary function usually ranges from a few eV to a few hundred eV and is overlapped with the region that the potential energy reaches during radiation damage processes. This is one of the reasons for the potential model dependence.

In this study, we develop an embedded atom method (EAM) potential model for pure bcc-Fe, which is the base structure of ferritic steels. Previous research [4] indicates that radiation damage in pure Fe is intrinsically similar to that in Fe alloy. To achieve a potential model that can reasonably reproduce both material properties and radiation damage, we construct a potential model in the form of a Fourier series and the model error is systematically minimized compared to the density functional theory (DFT) molecular dynamics calculation with various system. The performance of the developed potential model is verified in comparison with existing EAM potential model (HA-VD developed by Haftel and modified by Vascon [5] and AM2004 developed by Ackland [6]) and DFT calculation result.

## 2. Methods

### *2.1. Reference data by DFT calculation*

To accumulate the reference data to be used in the potential model construction, we performed DFT simulations with 3 × 3 × 3 supercells containing 54 atoms and a molecule system containing 2 atoms. Energy, force and stress data of 6750 configurations were obtained in total, including perfect crystals with equilibrium state and collision condition, defected crystals and strained crystals. To effectively accumulate the data, first-principles molecular dynamics (FPMD) was performed. The time step was 2 fs for equilibrium state and 1 fs for collision condition. The temperature ranged from 300 K to 2100 K (around melting point) for perfect crystal in equilibrium state, and the temperature for defected crystals was set to 300 K or 600 K. For the collision condition, the primary knock-on atom (PKA) energy was set to 40 eV or 100 eV.

To perform DFT calculation, Vienna *ab initio* simulation package (VASP) was used with the projector augmented-wave (PAW) method. The Perdew-Burke-Emzerhof (PBE) exchange correlation functional was utilized. The semi-core potential with 14 valence electrons ($Mg3p^6 4s^1 3d^7$) was used. The plane-wave cutoff energy was set to 293.2 eV, and 4 × 4 × 4 Monkhorst-Pack grid, which gives 36 irreducible k-points, was used for the k-point sampling.

### *2.2. Potential model*

We constructed an EAM potential model using energy, force and stress data generated by DFT calculations as the fitting reference. The potential model is described as follows:

$$E_{pot} = \sum_{n} \sum_{i=1}^{N_{atom}} \sum_{k=0}^{N_{EAM,basis}-1} a_{EAM,k} \cos\left(k \frac{\rho}{\rho_{\max}} \pi\right) + \frac{1}{2} \sum_{i,j}^{i \neq j, r_{ij} < r_{cut}} \sum_{k=0}^{N_{2B,basis}-1} a_{2B,k} \cos\left(k \frac{r}{r_{2B,cut}} \pi\right) \quad (1)$$

where subscripts $i$ and $j$ are each atom in system, subscript $n$ is the number of embedding energy function (= 2 in current study), $r_{ij}$ is the distance between atom $i$ and $j$, $r_{cut}$ is the cut-off radius of pairwise interaction (= 0.6 Å in current study), and $N_{EAM,basis}$ and $N_{2B,basis}$ (both are 60 in current study) are the numbers of cosine series for embedding energy and pairwise potential energy, respectively. $\rho$ and $\rho_{max}$ are the electronic density and maximum electronic density, respectively. The Fourier series coefficient $a_k$ is determined by minimizing the difference between potential model and DFT calculation by least square fitting.

### *2.3. Computational details for performance test*

For the performance test, we calculated several properties, such as dimer interaction, equilibrium state properties, defect properties and TDE. All CMD simulations were performed using the Large-scale Atomic/Molecular Massively Parallel Simulator (LAMMPS) code. The defect formation energy was calculated with 12 × 8 × 8 supercells (1536 ± 1 atoms), while defect migration energy was calculated with 8 × 8 × 8 supercells (1024 ± 1 atoms). The nudged elastic band (NEB) method was used to determine the defect migration energy.

The simulations for determining TDE were performed with 0 K and 30 K condition. 30 K simulations were used to determine an average TDE and 0 K simulations were used for comparison with DFT calculations. TDE is defined as the minimum kinetic energy that can form a Frenkel pair. The formation of defect was judged by Wigner-Seitz (WS) analysis using the LAMMPS Voro++ package. The simulation length was 5 ps for each simulation.

## 3. Results and discussion

### *3.1. Fitting quality*

A comparison of energies between values determined with the DFT calculation and those obtained with the constructed potential model is presented in Fig. 1. The constructed potential model shows good agreement. The errors in energy, force, stress compared with DFT calculation are 8.0 meV/atom, 0.19 eV/Å and 6.0 kbar, respectively.

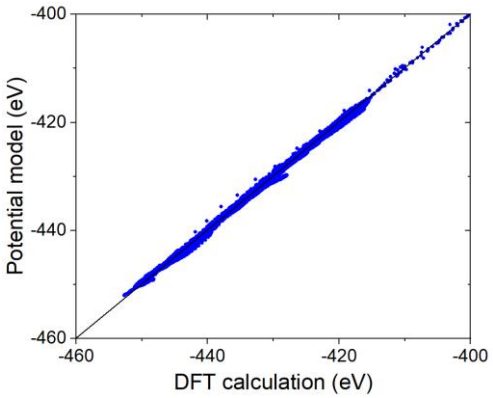


Fig. 1. Energy comparison between DFT calculation and the constructed potential model.

### *3.2. Potential shape*

Fig. 2 shows the Fe dimer interaction energy as a function of the interatomic distance. The potential shape of the constructed potential model is compared with ZBL, HA-VD and AM2004 potential models. The constructed potential model is reasonably similar to ZBL potential in a short range (< 0.7 Å).

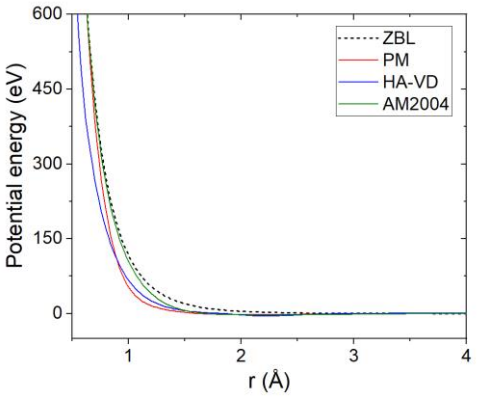


Fig. 2. Fe dimer interaction energy as a function of interatomic distance.

### *3.3. Material properties*

Performance test results with respect to material properties are summarized in Table 1. The constructed potential model reasonably predict lattice constant and bulk modulus compared to HA-VD and AM2004. For average TDE and defect formation energy, the constructed potential provide good agreement with DFT calculation, while the prediction of defect migration energy is just fair.

For TDE, displacement direction dependence was further investigated. The results are shown in Fig. 3 in comparison with results of DFT and HA-VD and AM2004 potential models. The prediction by the constructed potential model reasonably agree with DFT calculation.

These performance test results confirm that we have successfully constructed a potential model that can reasonably reproduce both material properties and radiation damage. Specifically, the constructed potential model nicely reproduces lattice constant, bulk modulus, average TDE and defect formation energy. Especially, TDE and defect formation energy are important for radiation damage simulations.

Table 1. Material properties predicted by DFT calculation and CMD calculation with three potential models. *a* is lattice constant, *K* is bulk modulus and $TDE_{avg}$ is average TDE.

| | DFT | PM | HA-VD | AM2004 |
|---|---|---|---|---|
| *a* (Å) | 2.83 | 2.83 | 2.87 | 2.86 |
| *K* (GPa) | 176 | 170 | 163 | 178 |
| $TDE_{avg}$ (eV) | 32 [a] | 34 | 35 | 40 |
| Defect formation energy (eV) | | | | |
| Vacancy | 2.2 | 1.8 | 1.4 | 1.7 [b] |
| SIA <110> | 4.4 | 4.4 | 6.7 | 3.5 [b] |
| SIA<111> | 5.3 | 4.7 | 6.9 | 4.0 [b] |

| Defect migration energy (eV) | | | | |
|---|---|---|---|---|
| $Vac_{1NN}$ | 0.67 [b] | 0.77 | 1.45 | 0.64 [b] |
| $SIA_{transl.}$ | 0.34 [b] | 0.15 | - | 0.31 [b] |

[a] Ref [7]
[b] Ref [8]

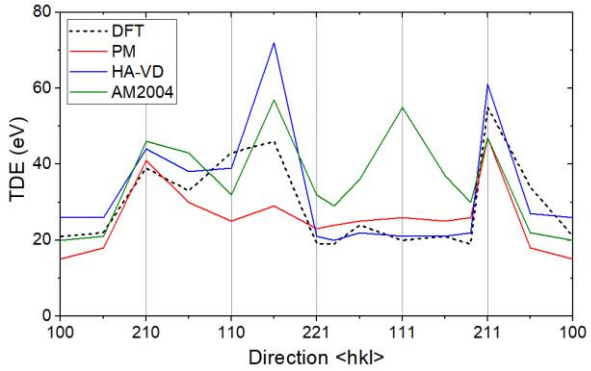


Fig. 3. TDE predictions along the boundary of the irreducible solid angle by DFT, PM, HA-VD, AM2004.

## 4. Conclusion

In this study, an EAM potential model of α-Fe was constructed using energy, force and stress data calculated by DFT. The constructed potential model reasonably agree with DFT results with respect to energy, force and stress in various conditions. We confirmed that the constructed potential model shows 0.004 %, 3.4 %, 6.3 % and 12.4 % errors in lattice constant, bulk modulus, TDE and defect formation energies, respectively, when compared to DFT results.

In a future work, we will evaluate the defect migration energies of other mechanisms such as rotation case for further performance test, and improve the constructed potential model in terms of defect formation and migration energies. By improving defect properties, we expect that the potential model becomes able to provide good performance in primary radiation damage calculation.

## 5. Acknowledgement

This research was supported by National Research Foundation (NRF) of Korea under Nuclear Research & Development Program by BK 21 plus project of Seoul National University.

## RFERENCES

[1] C. English, J. Hyde, Comprehensive Nuclear Materials, Elsevier, Vol. 4, pp. 151–180, 2012.
[2] B. Raj, M. Vijayalakshmi, Comprehensive Nuclear Materials, Elsevier, Vol. 4, pp. 97–121, 2012.
[3] K. Nordlund, J. Wallenius, L. Malerba, Molecular dynamics simulations of threshold displacement energies in Fe, Nucl. Instruments Methods Phys. Res. Sect. B Beam Interact. with Mater. Atoms, Vol. 246, No. 2, pp. 322-332, 2006.
[4] C. Björkas, K. Nordlund, L. Malerba, D. Terentyev, P. Olsson, Simulation of displacement cascades in Fe90Cr10 using a two band model potential, J. Nucl. Mater., Vol. 372, No. 2-3, pp. 312-317, 2008.
[5] R. VASCON, Cascades de deplacements atomiques dans le fer cubique centre, simulation par dynamique moleculaire, Thèse Dr. Phys. Paris 11 1997, pp. 164, 1997.
[6] G.J. Ackland, M.I. Mendelev, D.J. Srolovitz, S. Han, A. V Barashev, Development of an interatomic potential for phosphorus impurities in α-iron, J. Phys. Condens. Matter., Vol. 16, No. 27, pp. S2629-S2642, 2004.
[7] P. Olsson, C.S. Becquart, C. Domain, Ab initio threshold displacement energies in iron, Mater. Res. Lett., Vol. 4, No. 4, pp. 219–225, 2016.
[8] L. Malerba, M.C. Marinica, N. Anento, C. Björkas, H. Nguyen, C. Domain, F. Djurabekova, P. Olsson, K. Nordlund, A. Serra, D. Terentyev, F. Willaime, C.S. Becquart, Comparison of empirical interatomic potentials for iron applied to radiation damage studies, J. Nucl. Mater., Vol. 406, No. 1, pp. 19–38, 2010.